

# Portable Pesticide Electrochem-sensor: A Label-Free Detection of Glyphosate in Human Urine

Durgasha C. Poudyal,<sup>§</sup> Vikram Narayanan Dhamu,<sup>§</sup> Manish Samson, Sriram Muthukumar, and Shalini Prasad\*



Cite This: *Langmuir* 2022, 38, 1781–1790



Read Online

ACCESS |



Metrics & More

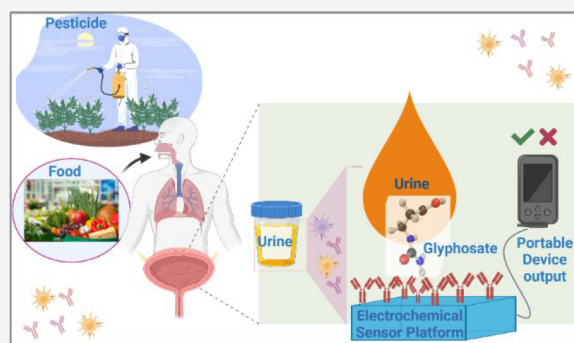


Article Recommendations



Supporting Information

**ABSTRACT:** The toxicity levels of and exposure to glyphosate, a widely used herbicide and desiccant, are significant public health issues. In this study, we aim to design a highly sensitive, label-free, portable sensor for the direct detection of glyphosate in human urine. The sensor platform consists of a portable, printed circuit board circular platform with gold working and reference electrodes to enable nonfaradic electrochemical impedance spectroscopy. The sensing platform was an immunoassay-based, gold electrode surface immobilized with a monolayer of dithiobis(succinimidyl propionate) (DSP), a thiol-based cross-linker, which was then modified with a glyphosate antibody (Glyp-Ab) through the bonding of the ester group of DSP with the amide of the antibody (Glyp-Ab). The sensor was tested electrochemically, first using the laboratory-based benchtop method for the glyphosate-spiked urine samples, resulting in a dynamic response in the concentration range of 0.1–72 ng/mL with a limit of detection of 0.1 ng/mL. The platform showed high selectivity in the presence of major interfering analytes in urine [malathion (Mal), 3-phenoxybenzoic acid (PBA), and chlorpyrifos (Chlp)] and high reproducibility. The sensing platform was then translated into a portable device that showed a performance correlation ( $r = 0.994$ ) with the benchtop (laboratory method). This developed portable sensing approach can be a highly reliable alternate sensor platform for the direct detection of pesticides in human bodily fluids.



## INTRODUCTION

Glyphosate is a well-known synthetic herbicide that was patented by the Monsanto Company in 1974 and is utilized in many products. Glyphosate is best known for its use in “Round-Up” pesticide products and is the herbicide that is used with Monsanto-branded GMOs.<sup>1–4</sup> The wide application of glyphosate and related herbicides has enhanced the growth of glyphosate resistant and tolerant weeds worldwide, consequently increasing applications at higher concentrations.<sup>1</sup> Glyphosate has also become the most used pesticide in the world, with the United States being responsible for nearly 19% of the global consumption of glyphosate.<sup>5</sup> However, glyphosate has been listed as a probable carcinogen by the International Agency for Research on Cancer and is being scrutinized by the scientific community because of its toxicity and ability to cause subtle but life-changing conditions.<sup>3,6</sup> Glyphosate operates by acting as an inhibitor of 5-enolpyruvylshikimate-3-phosphate synthase (EPSP synthase) not only in plants but also in bacteria.<sup>7</sup> Glyphosate has been directly linked with dysbiosis, a condition related to the imbalance between beneficial and deleterious bacteria. This can cause increased production of metabolites, which can contribute to the development of neurological conditions.<sup>7</sup> The use of glyphosate-based herbicides (GBHs) is directly related to the increase in the

level of homocysteine, which is a risk factor associated with cardiovascular disease.<sup>8</sup>

Due to the increasing use related to glyphosate tolerant plants, human exposure to it is inevitable through various sources such as bodies of water, agricultural runoff, food (dried pulses and cereals), and air.<sup>1</sup> The risk factors associated with long-term exposure to glyphosate make it important to minimize exposure. On the contrary, analyzing the exposure level at any time is critical for safety and clinical diagnosis.<sup>9</sup> Several regulatory authorities have established safe limits or concentrations of this herbicide in water and various food products we consume every day. The EU limit for glyphosate in water is 0.1  $\mu\text{g/L}$ , while the U.S. limit is 700  $\mu\text{g/L}$ .<sup>2</sup> For the evaluation of human exposure to glyphosate, in a study by the German environmental agency, a close group of young adults (in the years 2001–2015) were monitored, and of the 399 samples analyzed, roughly  $\sim 30\%$  showed glyphosate concen-

Received: October 28, 2021

Revised: January 18, 2022

Published: January 28, 2022



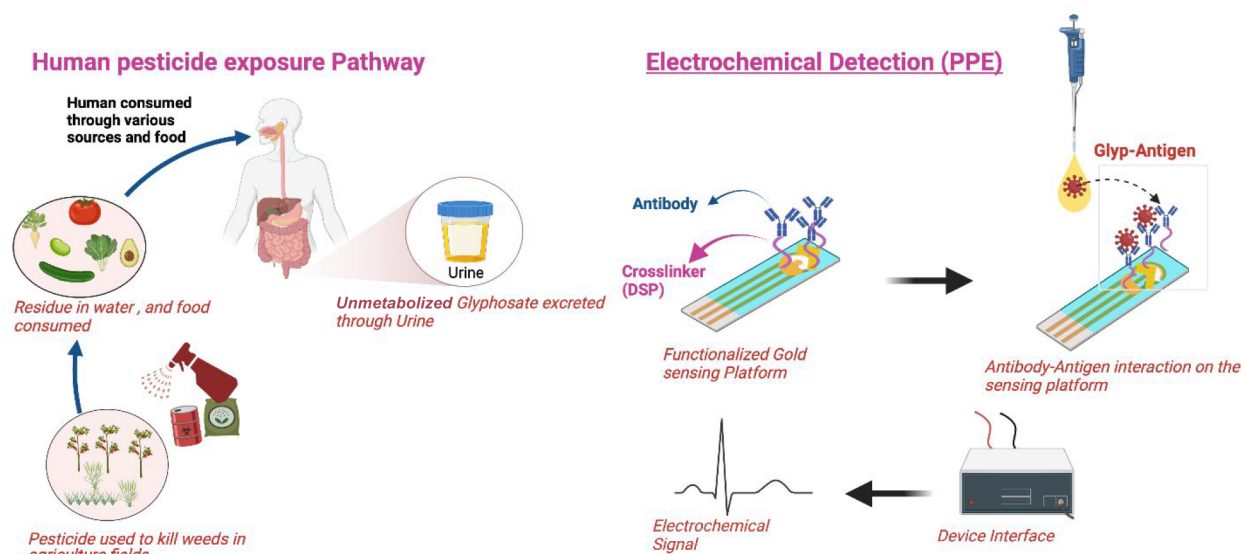


**Figure 1.** Schematic of the glyphosate residue in human urine and PPE (portable pesticide electrochem-sensor) sensing platform for direct detection of glyphosate in urine.

trations above the limit of quantitation ( $>0.1 \mu\text{g/L}$ ) analyzed via GC-MS.<sup>9</sup> A positive correlation has been reported between the urinary excretion of glyphosate and food consumption, which is important for biomonitoring in risk and safety assessments.<sup>10</sup> Increased levels of glyphosate in urine have been related to the level of bioavailable glyphosate absorbed by the body through various occupational sources and food residues. The absorbed glyphosate is poorly metabolized and is directly excreted in the urine and therefore can be measured in urine for risk assessment. The most recent analytical methods are highly sensitive and specific and claim to analyze glyphosate and other pesticides in human bodily fluids without the need for derivatization. These include, i.e., HPLC (high-performance liquid chromatography), FCMIA (fluorescence covalent microbead immunoassay), and LC-MS (liquid chromatography-mass spectrometry).<sup>1,11,12</sup> Current rapid detection systems such as enzyme-linked immunosorbent assays generally have high false positive and false negative rates, the industry protocol generally using LC-MS as a confirmation tool. The minimum limit of detection (LOD) is defined to be approximately  $2 \text{ ng/mL}$  when using LC-MS as an analysis tool.<sup>13</sup> Normally, this LOD is desirable for exposure-relevant concentrations, but it does not factor in degradation of food materials and the transfer of glyphosate from one medium to another.<sup>13</sup> For example, in the case of breast milk, glyphosate residue concentrations have been measured to be  $<1 \text{ ng/mL}$ , effectively nullifying the minimum LOD that is required by LC-MS to provide accurate results.<sup>14</sup> Using an even more specialized analytical method called triple-quadrupole LC-MS, 96.3% accuracy was achieved with a LOD of  $0.5 \text{ ng/mL}$ . All of these analytical methods require stringent preprocessing, specialized personnel, burdensome costs, and long processing times with no scope for on-field applications. The electrochemical methods are the most advanced to date for portable devices and on-field sensing applications.<sup>15,16</sup> Several electrochemical approaches for the detection of glyphosate have been reported.<sup>17</sup> Glyphosate is a non-electroactive compound, limiting its direct detection electrochemically. Several catalyst nanocomposites with or without the enzyme<sup>18</sup> have been used to improve sensitive and

selective detection through chemical interaction, formation of glyphosate–metal complexes and enzyme inhibition have been explored using, i.e., Cu-BTC MOF,<sup>17</sup> MMWCNTs-IL/CuO nanoparticles,<sup>19</sup> rGO-CuNPs composites,<sup>20</sup> a Cu-(poly)pyrrole composite,<sup>12,21</sup> SPE/Chi/CNO/TYR,<sup>22</sup> and n-Si/PANI/HRP.<sup>12,23</sup> A table of reported electrochemical sensor platform modifications and a comparison of responses is provided in Table S1. Most of these studies involve detection using a redox mediator through a faradic process employing a three-electrode system, complexation with the metal, or an enzyme inhibition method tested for food and water samples. A very low detection limit was also reported but involves sample preprocessing (Table S1). In addition to the sensitive analytical detection of glyphosate in human urine,<sup>24</sup> no data from direct analysis of the urine sample by the electrochemical method have been reported until now.

Another promising direct electroanalytical approach is electrochemical impedance spectroscopy (EIS) using the antibody-functionalized electrode to selectively detect the glyphosate antigen reported by our group in produce and food samples.<sup>25,26</sup> It is based on the measurement of the impedance over a wide range of frequencies, and the frequency domain response gives us useful information about the physicochemical changes that occur at the electrode surface as a result of the specific binding of an analyte or antigen of interest.<sup>25,26</sup> The previously reported work on the electrochemical method of detecting other pesticides used a diluted urine sample due to the complexity of the system,<sup>27</sup> which interfered with the faradic response. There have been no reports of a portable electrochemical device that can directly detect pesticides in urine. Developing a portable electrochemical device would be significant, especially with there being a burgeoning interest in rapid detection systems for the assessment of pesticides in urine.

Considering this background, in this work, we have fabricated a portable, label-free, on-field deployable, electrochemical sensor using working and reference electrodes as the sensor platform that is immobilized with the glyphosate antibody and linked with a cross-linker to directly detect the presence of glyphosate in urine as shown in Figure 1. The

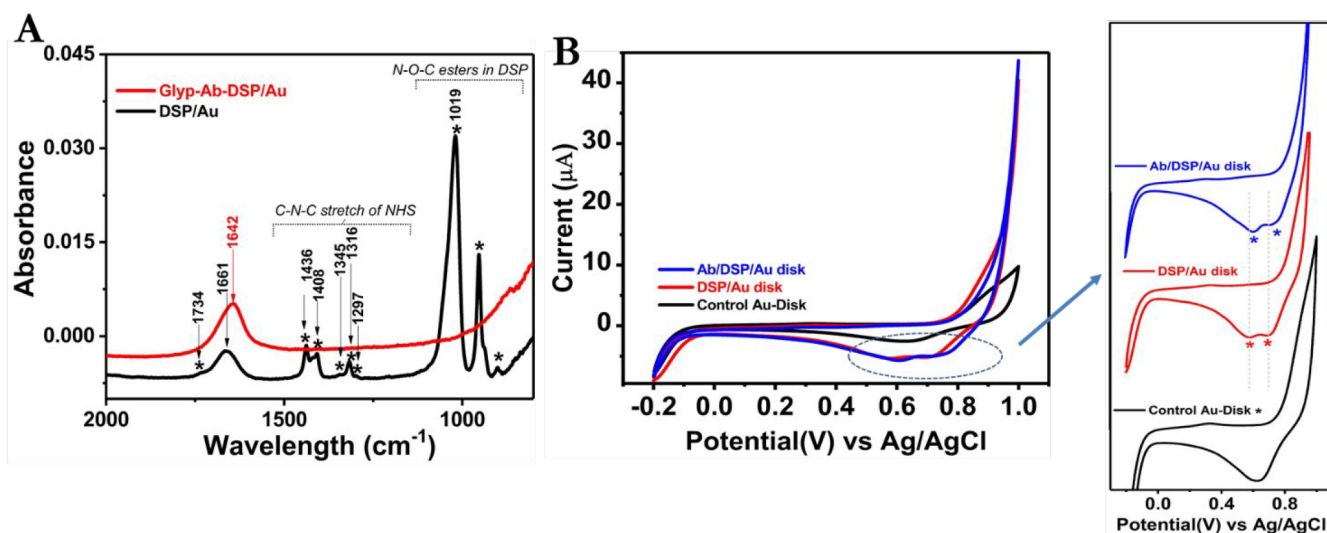


**Figure 2.** (A) FTIR spectra of the DSP cross-linker-immobilized gold substrate (black) and glyphosate antibody bound to a DSP gold substrate (red). (B) Electrochemical study of electrode surface modification using a three-electrode system in PBS (pH 7.4) and CV voltammetry of a control Au disk (black), a DSP/Au disk revealing two peaks due to DSP bound on the Au disk surface (red), and Ab-DSP/Au (blue).

interaction between the glyphosate antigen and antibody can be transduced as nonfaradic signals using EIS and CA (sampled on a millisecond time scale, which is the diffusion limited) measurement techniques. This selective and sensitive system should be viewed as a proof of concept and can be applied to future hand-held applications in real time of pesticides in various food products and human bodily fluids.

## EXPERIMENTAL SECTION

**Chemicals and Reagents.** Dithiobis(succinimidyl propionate) (Thermo Scientific), glyphosate antibody (Fitzgerald Antibodies), glyphosate antigen, chlorpyrifos, 3-phenoxybenzoic acid, dimethyl sulfoxide (DMSO), creatinine, sodium chloride, uric acid, and a phosphate-buffered saline solution (pH 7.4) were procured from Sigma-Aldrich. Malathion was procured from Cayman Chemicals. Normal urine collected from pooled donors was procured from Lee BioSolutions.

**Instrumentation.** A HIROX microscope (series RH 2000) was used to image the surface of the bare electrode, DSP, and the DSP-antibody-modified electrode surface. Fourier transform infrared (FTIR) spectroscopy was performed using the Nicolet iS50 FTIR spectrometer at spectral scans of 256 at 4  $\text{cm}^{-1}$  resolution in the wavelength range from 4000 to 600  $\text{cm}^{-1}$  to confirm the binding of the cross-linker and bonding of the glyphosate antibody to the gold electrode surface. All electrochemical measurements were performed using a Gamry Reference 600 potentiostat (GAMRY Instruments) and an EmstatPico modular system. The sensor platform consists of a portable printed circuit board circular platform with gold working and reference electrodes. The sensor design described above was printed on a PCB-FR4 substrate with ENIG gold finish on a copper-clad board as shown in panels A and B of Figure 3. All data and graphs were plotted using GraphPad Prism and Origin Pro 2017, and the graphical abstract and mechanism figures were drawn using Bio-Render and Adobe Illustrator.

**Electrochemical Surface Characterization of the Modified Sensing Platform.** To electrochemically understand the surface modification of the gold electrode, cyclic voltammetry and EIS were used employing the three-electrode system (using surface functionalization similar to that of the two-electrode sensing platform) in phosphate-buffered saline (PBS) (7.4) at each step of modification. A commercial Au disk (Metrohm, 2 mm diameter) was used as a working electrode, Ag/AgCl (saturated KCl) as a reference, and a Pt wire as the counter electrode. Prior to the experiment, the Au disk electrode was polished with a 0.05  $\mu\text{m}$  alumina slurry to create a

uniform surface roughness, followed by washing with a copious amount of Milli-Q water and potentiodynamic cycles in a potential window from  $-0.2$  to  $1.4$  V in  $0.5$  M  $\text{H}_2\text{SO}_4$  at a scanning rate of  $100$  mV/s until the characteristic hydrogen–oxygen adsorption–desorption peak in acid arises. Finally, the electrode was rinsed with water and kept in a desiccator for further use.

For the electrode modification, the cleaned Au disk electrode surface mentioned above was dispensed  $10$   $\mu\text{L}$  of  $10$  mM cross-linker dithiobis(succinimidyl propionate) (DSP) dissolved in DMSO. The electrode was then incubated at room temperature for  $90$  min, giving a sufficient reaction time for the immobilization of the cross-linker. The surface of the electrode was washed with PBS (twice) to remove unbound DSP, and electrochemical measurements were recorded using cyclic voltammetry (CV) (at a potential window from  $-0.2$  to  $1$  V) and EIS (AC bias of  $10$  mV, in the frequency range from  $1$  MHz to  $10$  Hz). The electrode was loaded with  $10$   $\mu\text{L}$  of a  $500$   $\mu\text{g}/\text{mL}$  glyphosate antibody solution and allowed to incubate for  $30$  min, and CV and EIS measurements were recorded for the resulting antibody-bound electrode surface. The validation of the chemisorption of the thiolated cross-linker DSP and binding of the glyphosate antibody was confirmed by the well-known FTIR analysis.

**Fabrication of the Electrode Sensing Platform for the Detection of Spiked Glyphosate in Human Urine.** The remodification of the electrode consists of washing the gold chip platform three times with isopropyl alcohol (IPA) followed by deionized water to remove the surface-adsorbed impurities.<sup>25,26</sup> After the sensor surface is deemed to be clean, the sensor was placed in a Faraday cage and  $180$   $\mu\text{L}$  of  $10$  mM DSP dissolved in DMSO was dispensed onto the gold electrode sensing region. The sensor chip was then allowed to incubate for  $90$  min (as discussed above). After the completion of the incubation period, EIS and CA measurements were recorded. The electrode surface was then washed twice with DMSO to remove any unbound DSP cross-linker remaining on the electrode surface followed by washing with a PBS solution. The surface of the sensor was then coated with  $20$   $\mu\text{L}$  per electrode of a  $500$   $\mu\text{g}/\text{mL}$  glyphosate antibody solution that was then allowed to incubate for  $30$  min. After incubation, EIS and CA measurements were taken using the lab instrument (potentiostat) and the data were recorded. The sensor surface was then washed with  $60$   $\mu\text{L}$  of PBS to remove any unbound antibody. Lastly,  $60$   $\mu\text{L}$  of Superblock (SB) was dispensed onto the electrode surface and incubated for  $10$  min to reduce the nonspecific binding by hydrolyzing the functional sites of DMSO. After the completion of the incubation period, EIS and CA measurements were taken, and the sensors were stored at  $4$   $^\circ\text{C}$ .

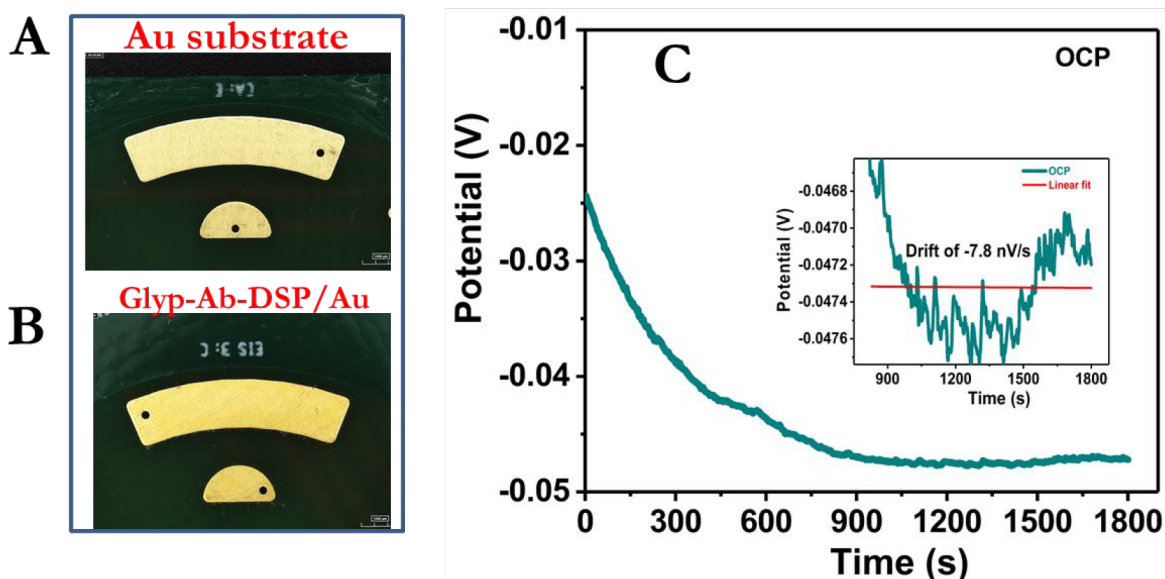


**Figure 3.** (A and B) HIROX images of the gold electrode sensor platform prior to and after functionalization with a cross-linker and Glyp-Ab antibody, respectively. (C) Open circuit potential of the functionalized sensor platform in the real urine sample measured for 30 min. The inset is the decay and/or drift of the sensor measured for the last 15 min of the stability test.

## RESULTS AND DISCUSSION

### Characterization of the Modified Sensing Platform.

The surface interaction or chemisorption of the thiolate cross-linker (DSP) to the gold surface and binding of the antibody to the cross-linker were confirmed using FTIR analysis. A gold thin film deposited on the glass surface by electron beam vapor deposition having a gold film similar to that of the sensing electrode platform was functionalized (as discussed in the sensor modification section), and absorbance values were recorded after the loading of the DSP cross-linker and the antibody. As shown in Figure 2A, the absorbance spectra of DSP-Au show binding of the cross-linker represented by the peak at  $1029\text{ cm}^{-1}$  characteristic of N–O–C esters in DSP, the peaks at  $\sim 1297$ ,  $1316$ ,  $1345$ ,  $1408$ , and  $1436\text{ cm}^{-1}$  corresponding to the C–N–C stretch of NHS esters, and the peak at  $1734\text{ cm}^{-1}$  representing the carbonyl stretching of NHS esters. When the antibody is immobilized on the cross-linker surface, the C–O bond of the ester reacts with the primary amines of the antibody forming stable amides.<sup>15,28</sup> The peaks due to NHS were masked, and an enhanced aminolysis peak at  $\sim 1642\text{ cm}^{-1}$  confirmed the successful binding of the glyphosate antibody.

As an approach for electrochemically validating the surface modification of the electrode, we used a three-electrode system using a commercial Au disk (2 mm diameter) as the working electrode in PBS (pH 7.4). As shown in Figure 2B, CV of the blank Au disk shows characteristic peaks due to oxygen adsorption and reduction at the gold electrode. After immobilization of DSP on Au (DSP/Au), CV reveals two reduction peaks at potentials of 0.568 and 0.705 V, which may be attributed to the DSP monolayer on the electrode through the S–Au (thiol–Au) interaction.<sup>29</sup> However, after the Glyp-Ab (antibody) had been loaded on the modified DSP/Au surface, the two peaks due to S–Au binding were observed at 0.601 and 0.730 V versus Ag/AgCl that shifted toward more positive potentials by 0.137 and 0.129 V, respectively, due to the binding of the Glyp-Ab on the DSP/Au surface. This characteristic binding phenomenon was also observed and can

be related to the EIS measurements (over a frequency range of 10–1000000 Hz at a 10 mV sinusoidal AC input signal) before and after the immobilization of cross-linker DSP and Glyp-Ab on the gold sensing electrode. As shown in panels A and B of Figure S1, the double-layer modulation due to the bound -SH monolayer on the electrode surface was observed as an increase in  $Z_{\text{mod}}$  (Bode plot) and capacitive behavior (Nyquist plot) when compared to the control gold electrode surface in PBS (7.4).

**Electrochemical Detection of Glyphosate Spiked in Real Human Urine Samples.** Panels A and B of Figure 3 show the optical (HIROX) images of the sensing platform before and after the modification. The Au electrode, after functionalization with the cross-linker DSP and glyphosate antibody (Glyp-Ab), revealed a thin layer of functionalized surface upon removal of the unbound DSP and antibody via PBS washing as shown in Figure 3B (bottom picture). After the functionalization step and successful binding of the cross-linker and Glyp-Ab to the electrode, the stability of the sensing platform was tested by measuring the open circuit potential of the pooled urine sample (real sample matrix for this study) to measure the inherent potential between the working and reference electrodes without any applied bias. As shown in Figure 3C, the initial shift in the potential in the time period from 0 to 900 s toward the negative side can be attributed to the adsorption of ions and/or metabolites present in urine. In addition, the potential stabilizes after 900–1800 s where the observed drift and/or decay was observed to be  $-7.8\text{ nV/s}$ . Therefore, the initial incubation period of 30 min (1800 s) was maintained for the control urine sample for this study to allow the system to stabilize.

Nonfaradic EIS (at a small, applied AC bias of 10 mV) and chronoamperometry (at a 0.5 V applied bias in the nonfaradic region at the  $<20\text{ ms}$  time scale) were used to record the signal response of this sensing device. The small, applied bias caused electrical double-layer formation at the electrode–electrolyte interface. The modulation of the double layer due to the binding of the target antigen to the antibody-modified

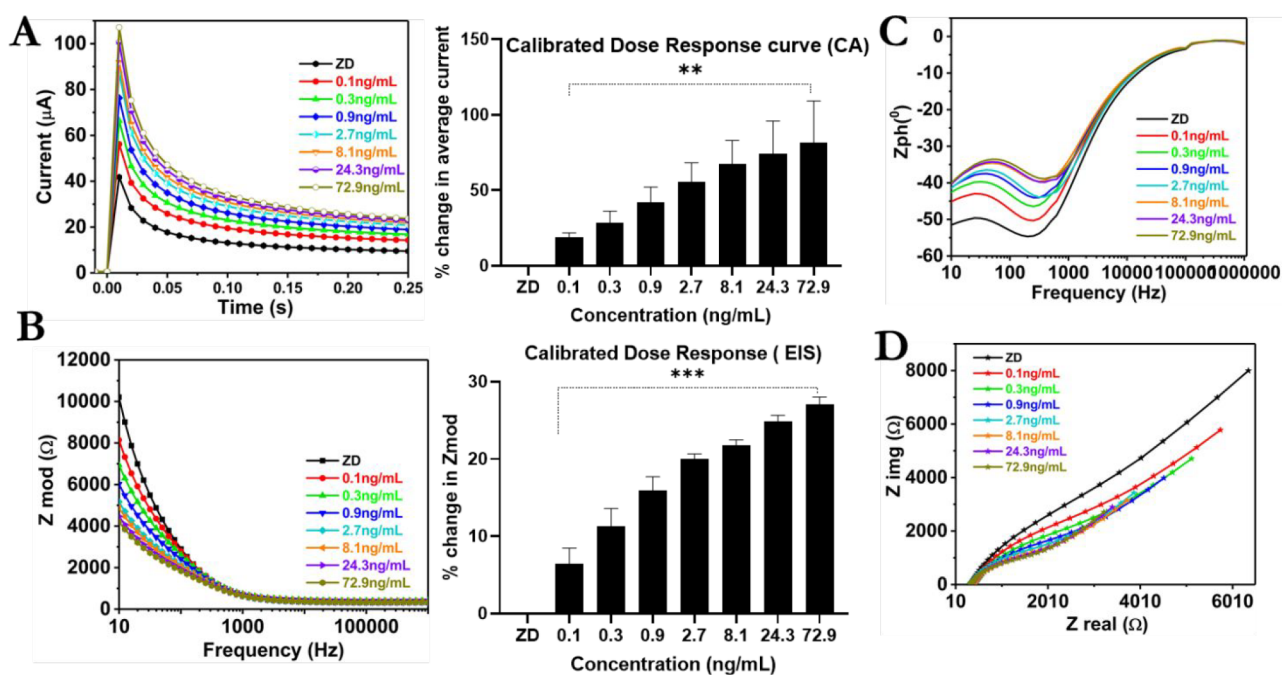


**Figure 4.** Electrochemical performance of the sensor using a laboratory benchtop instrument. (A) Chronoamperometry (CA) response for the control urine (ZD) and spiked concentration of glyphosates (0.1–72.9 ng/mL) in urine and its characteristic calibrated dose response (CDR) plot. (B) Bode response and characteristics CDR. (C and D) Phase and Nyquist data for glyphosate spiked in pooled human urine.

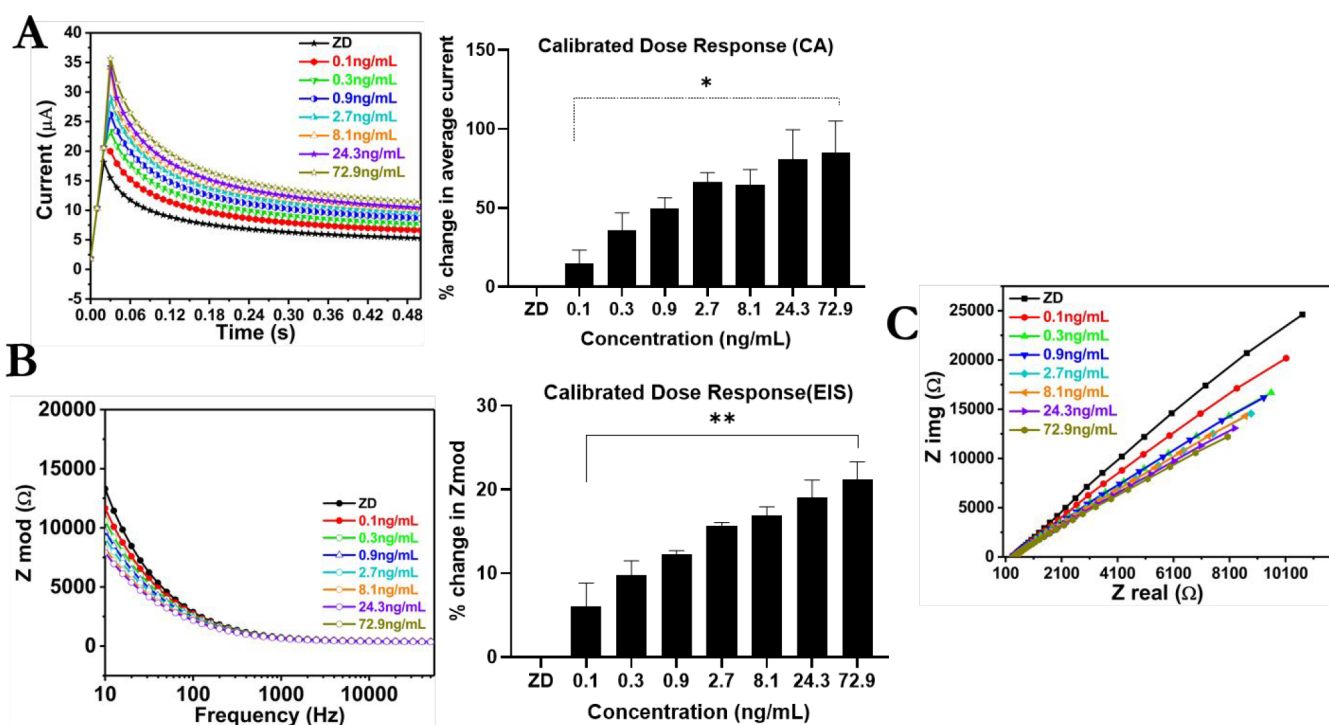


**Figure 5.** Electrochemical performance of the sensor using a portable sensing device. (A) Chronoamperometry (CA) response for the control urine (ZD) and spiked concentrations of glyphosates (0.1–72.9 ng/mL) in urine and its characteristic calibrated dose response (CDR) plot. (B) Bode plot and its characteristic CDR. (C) Nyquist data for spiked glyphosate in pooled human urine.

electrodes resulted in the signal arising in the form of a change in the  $Z_{\text{mod}}$  value in EIS and the nonfaradic current in the chronoamperometry.

**Calibrated Dose Response Measurement of the Spiked Glyphosate in Urine Samples Using a Sensing Platform.** Normal urine from pooled donors (Lee Bio-Solutions) was utilized as the primary matrix for the spiking

experiment as well as the aqueous solvent for the concentration samples. EIS and CA, a nonfaradic electrochemical method, were used as the measurement tool to gauge the response of the sensor owing to the antibody–antigen interaction at the sensing platform. All of the measurements were recorded first with the laboratory benchtop instrument followed by the portable electrochemical device for all of the study. To prepare

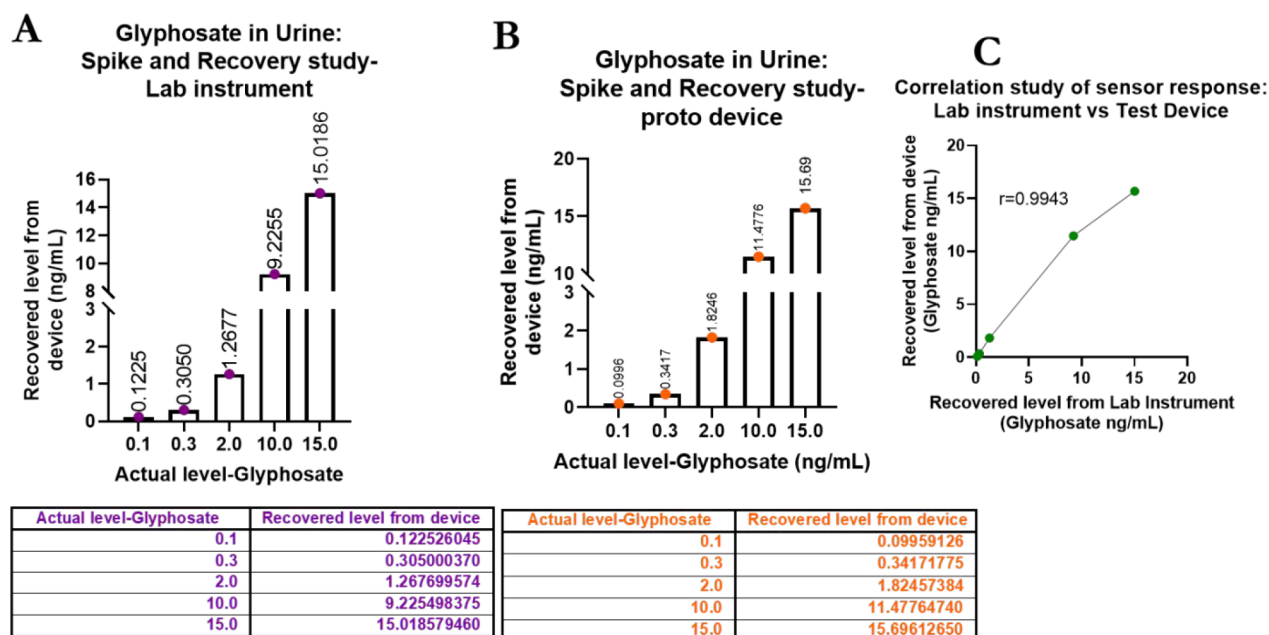


**Figure 6.** (A and B) Spike and recovery data for glyphosate spiked in urine for a lab benchtop device and a portable electrochemical device, respectively. (C) Comparison of the performance of the two-device (portable device on the y-axis and lab instrument on the x-axis) method by Pearson correlation of the developed label-free sensing platform.

the spiked calibrated dose measurements (CDR), the concentrations of the glyphosate antigen ranged from 0.1 to 72.9 ng/mL. This was done by serial dilution of the stock solution of pooled urine from human donors. The zero dose (ZD/control dose with no spiked glyphosate antigen) was dispensed onto the electrode surface and allowed to incubate for 30 min. After the incubation period, EIS and CA were performed. The zero-dose liquid was then slowly removed from the electrode surface via pipet. The 0.1 ng/mL dose was then dispensed onto the electrode surface and allowed to incubate for 12 min before EIS and CA tests were run and the data were recorded. An incubation/reaction time of 12 min was there to allow sufficient binding of the antigens to the electrode surface and was maintained for all of the experiments. This procedure was repeated for the remaining doses of 0.3, 0.9, 2.7, 8.1, 24.3, and 72.9 ng/mL.

Figure 4A shows the CA plot in which the change in the current (microamperes) was plotted versus time (seconds); with an increasing concentration, the current increased from 41.5 to 106.9  $\mu\text{A}$  at a time scale of <20 ms for the added spiked doses with 0.1–72.9 ng/mL glyphosate. The observed signal in the form of current is attributed to the double-layer modulation due to the binding of the antigen to the antibody. The percentage change in peak current from the baseline (at  $\sim 10$  ms) was plotted versus the subsequent added concentration of spiked glyphosate to obtain the calibrated dose curve (calibration curve). Figure 4B also shows the nonfaradic sensing data using EIS represented in the form of the Bode plot; the  $Z_{\text{mod}}(\Omega)$  plotted against the frequency (hertz) shows the signal response in the form of a decreasing  $Z_{\text{mod}}(\Omega)$  value of 2896  $\Omega$  for the baseline (ZD) to 1835  $\Omega$  as a function of the interaction of the antigen with the antibody in the frequency range of 10–10<sup>6</sup> Hz.

The percentage change in the  $Z_{\text{mod}}$  value at one frequency (100 Hz) was extracted, and the value was plotted versus the spike concentration of glyphosate to obtain the CDR plot (calibration plot) for the replicates (average of three chips

consisting of 18 electrodes) as shown in the column graph in Figure 4B (right). Panels C and D of Figure 4 represent the characteristic Z phase change from  $-53^\circ$  to  $34.5^\circ$  and a Nyquist plot ( $Z_{\text{img}}$  vs  $Z_{\text{real}}$ ) that correlated the electrode surface charge modulation as a function of an increasing dosing (0.3–72.9 ng/mL) to the increasing level of binding of the antigen to the antibody.

As a proof of concept study for the possible miniaturization of this sensing platform, all of the electrochemical measurements were performed using a laboratory benchtop instrument (data shown in Figure 5) and restudied and/or repeated on the portable electrochemical device setup using the same sensing platform. As shown in Figure 5A, the representative chronoamperometry signal shows an increase in current from 18.3 to 35.73  $\mu\text{A}$ . The corresponding CDR plot was obtained by plotting the percentage change in the average current from the control or zero-dose solution (an average of  $N = 18$  was considered) with respect to the increasing concentration of spiked glyphosate in real urine.

Similar to the benchtop lab instrument data, the EIS signal observed on the portable device showed a decrease in the raw  $Z_{\text{mod}}$  value from 2877 to 2177  $\Omega$  for the ZD/control urine, 0.1–72.9 ng/mL dose of spiked glyphosate. A characteristic CDR plot was obtained (Figure 5B, right) by extracting the signal response at 100 Hz (the best response was observed at this frequency) in the form of the percentage change in  $Z_{\text{mod}}$  from the baseline (control dose). Similarly, the Nyquist plot as shown in Figure 5C was bending toward a higher  $Z_{\text{real}}$  due to the binding of more antigen on the electrode surface with an increase in dose.

**Spike and Recovery and Correlation Study between the Benchtop and Portable Device.** The efficacy of the sensor and portable device in examining glyphosate levels in urine was evaluated by measuring the randomly picked concentration within the calibrated dose range on the sensor and determining the recovered concentration doses from the calibration curve as shown in panels A and B of Figure 6 for

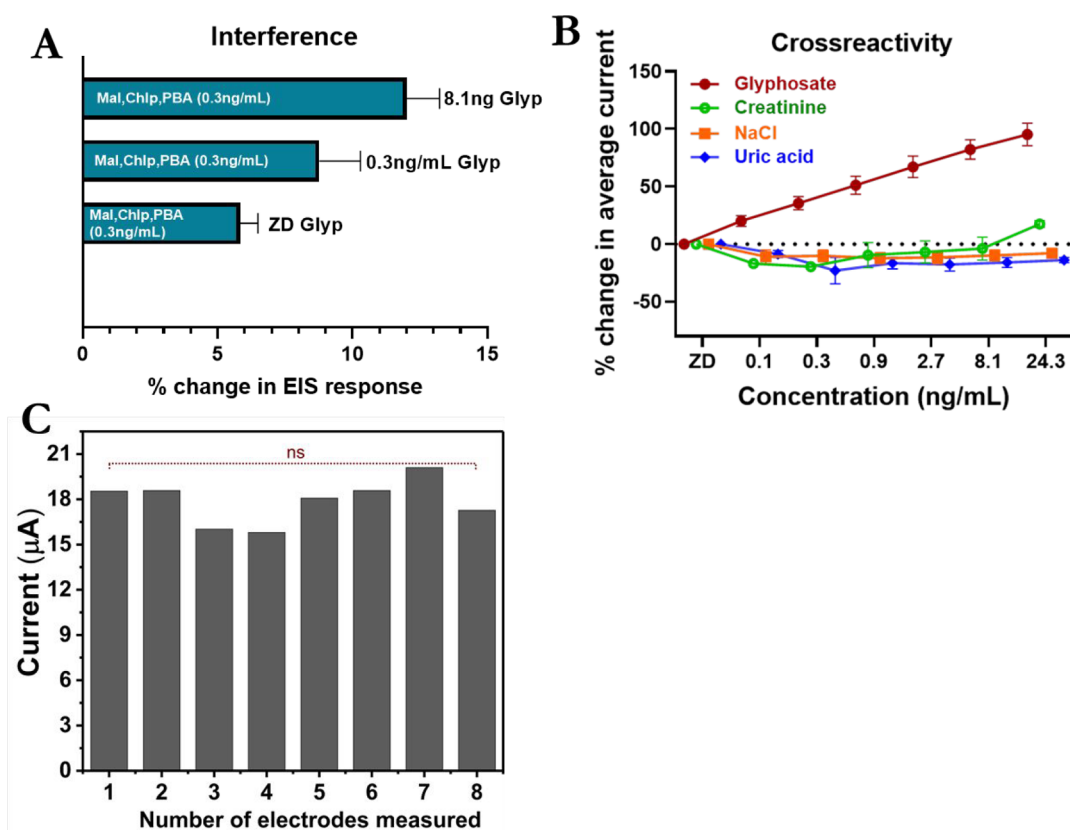


**Figure 7.** (A) Interference study representing the change in the EIS response for the spiked concentration of three common interfering ions (Mal, Chlp, and PBA) with ZD glyphosate, 0.3 ng/mL glyphosate, and 8.1 ng/mL glyphosate. (B) Cross reactivity measured on the basis of the percent change in the current of Glyph compared with the interfering analyte creatinine, NaCl, and uric acid present in urine. (C) Representative reproducibility response plot for 0.9 ng/mL glyphosate spiked in urine, measured with eight electrodes using chronoamperometry (\*ns = nonsignificant with  $p > 0.05$ ).

both the lab instrument and portable device, respectively. The regression fitting for the calibrated dose response for the back-calculated recovery dose is shown in Figure S2. As one can see in these consolidated data plots (Figure 6), the sensor shows a sensitive response with a limit of detection (LOD) as low as 0.01 ng/mL (1 ppb), which is the lowest detectable range above the specific signal threshold (SST) equivalent to those of both the portable device and the lab potentiostat device and an upper limit range of 15 ng/mL (15 ppb), and the CDR shows a response of  $\leq 72.9$  ng/mL (72.9 ppb). Upon analysis of the actual versus recovered concentrations on each instrument shown in the bottom tables of panels A and B of Figure 6, the concentration of the recovery was desirable and falls within the 80–110% estimation rate with no directional bias on either side; i.e., the system does not overpredict or underpredict every single time. An additional performance metric of the test system was determined by correlating the results obtained on the portable device against those of the reference lab instrument as shown in Figure 6C. The parametric test via Pearson correlation analysis was performed between the recovered results of the two methods to survey the sensor toward point-of-use deployability. This was done by running a parametric bivariate correlation test based on linear matching between the test device data set on the  $y$ -axis and the lab instrument results on the  $x$ -axis in Figure 6C. The extracted Pearson correlation coefficient ( $r = 0.9943$ ) was observed denoting excellent correlation between the results for the glyphosate pesticide from the two devices. Therefore, from the

experimental cycles described above and their respective analysis, it was understood that the functionality of the proposed sensor system depicted a high consensus with the actual spiked concentration value of the pesticide, and further correlation of the data with a standard lab instrument indicated the ability of our developed label-free sensor platform to translate into a portable field electroanalytical device.

**Selectivity, Reproducibility, and Stability Test.** The response of nonspecific analytes such as malathion (Mal), chlorpyrifos (Chlp), and 3-phenoxybenzoic acid (PBA), major interfering analytes found in the urine, was tested using CA. As shown in Figure 7A, the change in the EIS response for the spiked concentration of three interfering ions (Mal, Chlp, and PBA) was observed to be  $5.8 \pm 0.93\%$ , the response of the 0.3 ng/mL glyphosate showed a response of  $8.7 \pm 1.2\%$ , and further addition of 8.1 ng/mL glyphosate showed the response to be 12% as calculated from the ZD (control urine). The effects of other biomolecules and ion interfering analytes present in urine such as creatinine, uric acid, and sodium salt toward the signal response were compared to those of the target analyte for the sensor platform as shown in Figure 7B. The percent change in the current response was extracted from the CA study for the 0.1–24.3 ng/mL interfering analyte concentration spiked in urine. The sodium salt and uric acid showed no positive responses; however, creatinine at small doses (0.1–0.9 ng/mL) showed a negative response, whereas at higher concentrations (2.7–24.3 ng/mL), the percent change in the observed current was 1.82–17.51%. This study

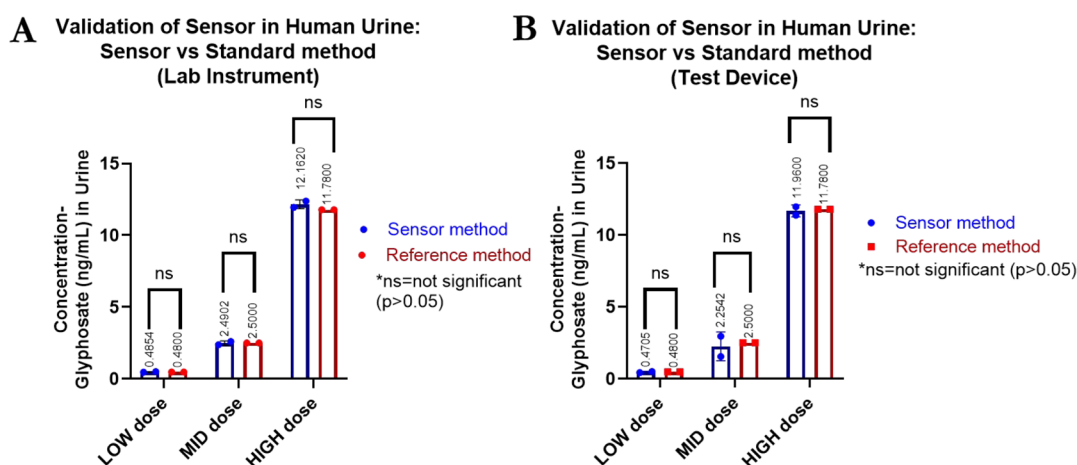


**Figure 8.** Validation of blinded spiked low-, medium-, and high-dose urine samples using (A) comparison of a laboratory instrument to the standard method (reference) and (B) developed PPE sensing platform compared to the standard reference method.

confirms that even in the presence of interfering analytes, the sensor can respond at smaller doses. Figure 7C shows the representative plot for the reproducibility of the sensors tested for 0.9 ng/mL Glyp spiked in urine, measured using CA. The raw current value for eight electrodes ( $N = 8$ ) dosed with 0.9 ng/mL glyphosate showed an average current of  $17.8 \pm 1.7 \mu\text{A}$ , confirming the high reproducibility of the sensors across eight electrodes (ns, with  $p > 0.05$ ).

To examine the stability, in terms of the life of the sensing platforms, a batch of sensors (more than six) were prepared and functionalized in a day with the antibody and superblock (as discussed in the section about the fabrication of the electrode sensing platform) and stored at  $4^\circ\text{C}$ . Prior to use, the sensing platforms were removed from the refrigerator and kept at room temperature for approximately 10–15 min. Therefore, the data obtained for the calibrated dose response (see Figures 4 and 5) consist of an average of 18 electrodes, and the data were collected for every three chips on different days over a week, which showed results within a  $<20\%$  error on the response. The prepared sensor platform response is based on antibody–antigen binding, which is an irreversible binding process, optimized to detect the low concentration dose of glyphosate, and therefore, it was used only once and was not reused or reusable.

**Cross Validation of Glyphosate in Human Urine Samples (single-blind study).** Cross-validation was performed by a standard laboratory analysis method (UPLC) on the same samples (three samples across different ranges of glyphosate in urine: LOW, MID, and HIGH) by a third-party group (INSPQ Canada). The measurements taken on the portable device system were translated back to the glyphosate concentrations (nanograms per milliliter or parts per billion) from the chronoamperometry-based calibration model as discussed above. This was compared and cross-referenced with the values retrieved from the standard method as a single-blind study.

The results from this cross-validation experiment are depicted in panels A and B of Figure 8 for the laboratory instrument and portable device, respectively. The sensor method data are marked by a blue border, and the reference method data are colored red. One can see from the bar plots with error bars (mean  $\pm$  standard deviation) that the intermethod variability or error is  $<10\%$  and the standard deviation that is representative of sensor-to-sensor variability

(intramethod variation) also falls within the range of  $\pm 15\%$ . Additionally, a two-tailed  $t$  test was performed on this data set to check for statistical significance between the two methods, and with a resulting  $p$  value of  $>0.05$ , it showed that no significant difference could be observed. Therefore, the sensor system could be assessed with a great degree of accuracy and precision be utilized to track glyphosate pesticide levels in human urine and possesses an increased potential for application in bioanalytical devices/point-of-care (POC) platforms.

## CONCLUSIONS

In this study, we demonstrate for the first time the detection of glyphosate spiked in a real human urine sample with a label-free, affinity-based electrochemical sensor consisting of a two-electrode sensing platform. The electrochemical nonfaradic response of the sensor as a function of the binding of the target antigen to the antibody-modified sensing platform showed a dynamic response in the concentration range of 0.1–72.9 ng/mL. The sensor had a detection limit of 0.1 ng/mL (three standard deviations of blank measurements). The sensing platform showed a high selectivity for glyphosate in the presence of major interfering analytes, i.e., malathion (Mal), 3-phenoxybenzoic acid (PBA), and chlorpyrifos (Chlp), with similar structural properties and biomolecules, i.e., creatinine, uric acid, and sodium salts found in urine. The sensor showed a high reproducibility for the three replicates (three chips across 18 electrodes). The portable pesticide electrochemical sensor (PPE) was successfully tested for translation using the portable electrochemical device showing a correlation coefficient  $r$  of 0.994 as compared with the laboratory benchtop method. Lastly, the PPE sensing platform was validated to test the blind samples for glyphosate at low, medium, and high doses of urine using both the laboratory benchtop instrument and the portable test device. This portable label-free sensing approach can be an alternate electrochemical tool for measuring pesticides in human fluids

## ASSOCIATED CONTENT

### Supporting Information

The Supporting Information is available free of charge at <https://pubs.acs.org/doi/10.1021/acs.langmuir.1c02877>.



Electrochemical study of the surface functionalization by EIS, regression analysis or fitting of the calibrated dose responses, and comparison of electrochemical sensors for glyphosate detection (PDF)

## AUTHOR INFORMATION

### Corresponding Author

**Shalini Prasad** – Department of Bioengineering, The University of Texas at Dallas, Richardson, Texas 75080, United States; EnLiSense LLC, Allen, Texas 75013, United States; [orcid.org/0000-0002-2404-3801](https://orcid.org/0000-0002-2404-3801); Phone: +1 (972) 883-4247; Email: [shalini.prasad@utdallas.edu](mailto:shalini.prasad@utdallas.edu)

### Authors

**Durgasha C. Poudyal** – Department of Bioengineering, The University of Texas at Dallas, Richardson, Texas 75080, United States; [orcid.org/0000-0002-7361-9395](https://orcid.org/0000-0002-7361-9395)

**Vikram Narayanan Dhamu** – Department of Bioengineering, The University of Texas at Dallas, Richardson, Texas 75080, United States

**Manish Samson** – Department of Bioengineering, The University of Texas at Dallas, Richardson, Texas 75080, United States

**Sriram Muthukumar** – EnLiSense LLC, Allen, Texas 75013, United States; [orcid.org/0000-0002-8761-7278](https://orcid.org/0000-0002-8761-7278)

Complete contact information is available at:

<https://pubs.acs.org/10.1021/acs.langmuir.1c02877>

### Author Contributions

<sup>§</sup>D.C.P. and V.N.D. contributed equally to this work.

### Notes

The authors declare the following competing financial interest(s): S.P. and S.M. have a significant interest in EnLiSense LLC, a company that may have a commercial interest in the results of this research and technology. The potential individual conflict of interest has been reviewed and managed by The University of Texas at Dallas and played no role in the study design; in the collection, analysis, and interpretation of data; in the writing of the report; or in the decision to submit the report for publication.

## REFERENCES

- (1) Gillezeau, C.; Van Gerwen, M.; Shaffer, R. M.; Rana, I.; Zhang, L.; Sheppard, L.; Taioli, E. The Evidence of Human Exposure to Glyphosate: A Review. *Environ. Heal. A Glob. Access Sci. Source* **2019**, *18* (1), 1–14.
- (2) Uka, B.; Kieninger, J.; Urban, G. A.; Weltin, A. Electrochemical Microsensor for Microfluidic Glyphosate Monitoring in Water Using MIP-Based Concentrators. *ACS Sensors* **2021**, *6* (7), 2738–2746.
- (3) Mesnage, R.; Defarge, N.; Spiroux de Vendômois, J.; Séralini, G. E. Potential Toxic Effects of Glyphosate and Its Commercial Formulations below Regulatory Limits. *Food Chem. Toxicol.* **2015**, *84*, 133–153.
- (4) Singh, S.; Kumar, V.; Datta, S.; Wani, A. B.; Dhanjal, D. S.; Romero, R.; Singh, J. Glyphosate Uptake, Translocation, Resistance Emergence. In *Crops, Analytical Monitoring, Toxicity and Degradation: A Review*; Springer International Publishing, 2020; Vol. 18.
- (5) Mills, P. J.; Kania-Korwel, I.; Fagan, J.; McEvoy, L. K.; Laughlin, G. A.; Barrett-Connor, E. Excretion of the Herbicide Glyphosate in Older Adults between 1993 and 2016. *JAMA - J. Am. Med. Assoc.* **2017**, *318* (16), 1610–1611.
- (6) Gasnier, C.; Dumont, C.; Benachour, N.; Clair, E.; Chagnon, M. C.; Séralini, G. E. Glyphosate-Based Herbicides Are Toxic and Endocrine Disruptors in Human Cell Lines. *Toxicology* **2009**, *262* (3), 184–191.
- (7) Rueda-Ruzafa, L.; Cruz, F.; Roman, P.; Cardona, D. Gut Microbiota and Neurological Effects of Glyphosate. *Neurotoxicology* **2019**, *75*, 1–8.
- (8) Hu, J.; Lesseur, C.; Miao, Y.; Manservigi, F.; Panzacchi, S.; Mandrioli, D.; Belpoggi, F.; Chen, J.; Petrick, L. Low-Dose Exposure of Glyphosate-Based Herbicides Disrupt the Urine Metabolome and Its Interaction with Gut Microbiota. *Sci. Rep.* **2021**, *11* (1), 1–10.
- (9) Conrad, A.; Schröter-Kermani, C.; Hoppe, H. W.; Rütther, M.; Pieper, S.; Kolossa-Gehring, M. Glyphosate in German Adults – Time Trend (2001 to 2015) of Human Exposure to a Widely Used Herbicide. *Int. J. Hyg. Environ. Health* **2017**, *220* (1), 8–16.
- (10) Soukup, S. T.; Merz, B.; Bub, A.; Hoffmann, I.; Watzl, B.; Steinberg, P.; Kulling, S. E. Glyphosate and AMPA Levels in Human Urine Samples and Their Correlation with Food Consumption: Results of the Cross-Sectional KarMeN Study in Germany. *Arch. Toxicol.* **2020**, *94* (5), 1575–1584.
- (11) Stalikas, C. D.; Konidari, C. N. Analytical Methods to Determine Phosphonic and Amino Acid Group-Containing Pesticides. *J. Chromatogr. A* **2001**, *907* (1–2), 1–19.
- (12) Zambrano-Intriago, L. A.; Amorim, C. G.; Rodríguez-Díaz, J. M.; Araújo, A. N.; Montenegro, M. C. B. S. M. Challenges in the Design of Electrochemical Sensor for Glyphosate-Based on New Materials and Biological Recognition. *Sci. Total Environ.* **2021**, *793*, 148496.
- (13) Krause, J. L.; Haange, S. B.; Schäpe, S. S.; Engelmann, B.; Rolle-Kampczyk, U.; Fritz-Wallace, K.; Wang, Z.; Jehmlich, N.; Türkowski, D.; Schubert, K.; Pöppe, J.; Bote, K.; Rösler, U.; Herberth, G.; von Bergen, M. The Glyphosate Formulation Roundup® LB plus Influences the Global Metabolome of Pig Gut Microbiota in Vitro. *Sci. Total Environ.* **2020**, *745*, 140932.
- (14) Steinborn, A.; Alder, L.; Michalski, B.; Zomer, P.; Bendig, P.; Martinez, S. A.; Mol, H. G. J.; Class, T. J.; Costa Pinheiro, N. Determination of Glyphosate Levels in Breast Milk Samples from Germany by LC-MS/MS and GC-MS/MS. *J. Agric. Food Chem.* **2016**, *64* (6), 1414–1421.
- (15) Jagannath, B.; Lin, K. C.; Pali, M.; Sankhala, D.; Muthukumar, S.; Prasad, S. Temporal Profiling of Cytokines in Passively Expressed Sweat for Detection of Infection Using Wearable Device. *Bioeng. Transl. Med.* **2021**, *6* (3), 1–14.
- (16) Tanak, A. S.; Jagannath, B.; Tamrakar, Y.; Muthukumar, S.; Prasad, S. Non-Faradaic Electrochemical Impedimetric Profiling of Procalcitonin and C-Reactive Protein as a Dual Marker Biosensor for Early Sepsis Detection. *Anal. Chim. Acta X* **2019**, *3*, 100029.
- (17) Cao, Y.; Wang, L.; Shen, C.; Wang, C.; Hu, X.; Wang, G. An Electrochemical Sensor on the Hierarchically Porous Cu-BTC MOF Platform for Glyphosate Determination. *Sens. Actuators, B* **2019**, *283*, 487–494.
- (18) Lee, J. K.; Park, S. H.; Lee, E. Y.; Kim, Y. J.; Kyung, K. S. Development of an Enzyme-Linked Immunosorbent Assay for the Detection of the Fungicide Fenarimol. *J. Agric. Food Chem.* **2004**, *52* (24), 7206–7213.
- (19) Gholivand, M. B.; Akbari, A.; Norouzi, L. Development of a Novel Hollow Fiber- Pencil Graphite Modified Electrochemical Sensor for the Ultra-Trace Analysis of Glyphosate. *Sens. Actuators, B* **2018**, *272*, 415–424.
- (20) Setznagl, S.; Cesarino, I. Copper Nanoparticles and Reduced Graphene Oxide Modified a Glassy Carbon Electrode for the Determination of Glyphosate in Water Samples. *Int. J. Environ. Anal. Chem.* **2022**, *102*, 293–305.
- (21) Shrivastava, S.; Kumar, A.; Verma, N.; Chen, B. Y.; Chang, C. T. Voltammetric Detection of Aqueous Glyphosate on a Copper and Poly(Pyrrole)-Electromodified Activated Carbon Fiber. *Electroanalysis* **2021**, *33* (4), 916–924.
- (22) Sok, V.; Fragoso, A. Amperometric Biosensor for Glyphosate Based on the Inhibition of Tyrosinase Conjugated to Carbon Nano-Onions in a Chitosan Matrix on a Screen-Printed Electrode.

*Microchim. Acta* **2019**, *186* (8), 569 DOI: 10.1007/s00604-019-3672-6.

(23) Roman, R. L.; Nagi, L.; Silva, L. L.; Fernandes, S. C.; de Mello, J. M. M.; Magro, J. D.; Fiori, M. A. Monocrystalline Silicon/Polyaniline/Horseradish Peroxidase Enzyme Electrode Obtained by the Electrodeposition Method for the Electrochemical Detection of Glyphosate. *J. Mater. Sci. Mater. Electron.* **2020**, *31* (12), 9443–9456.

(24) Niemann, L.; Sieke, C.; Pfeil, R.; Solecki, R. A Critical Review of Glyphosate Findings in Human Urine Samples and Comparison with the Exposure of Operators and Consumers. *J. fur Verbraucherschutz und Leb.* **2015**, *10* (1), 3–12.

(25) Dhamu, V. N.; Prasad, S. ElectrochemSENSE: A Platform towards Field Deployable Direct on-Produce Glyphosate Detection. *Biosens. Bioelectron.* **2020**, *170*, 112609.

(26) Dhamu, V. N.; Poudyal, D. C.; Muthukumar, S.; Prasad, S. A Highly Sensitive Electrochemical Sensor System to Detect and Distinguish Between Glyphosate and Glufosinate. *J. Electrochem. Soc.* **2021**, *168* (5), 057531.

(27) Geremedhin, W.; Amare, M.; Admassie, S. Electrochemically Pretreated Glassy Carbon Electrode for Electrochemical Detection of Fenitrothion in Tap Water and Human Urine. *Electrochim. Acta* **2013**, *87*, 749–755.

(28) Stevenson, H.; Bacon, A.; Joseph, K. M.; Gwandaru, W. R. W.; Bhide, A.; Sankhala, D.; Dhamu, V. N.; Prasad, S. A Rapid Response Electrochemical Biosensor for Detecting Thc In Saliva. *Sci. Rep.* **2019**, *9* (1), 1–11.

(29) Pensa, E.; Cortés, E.; Corthey, G.; Carro, P.; Vericat, C.; Fonticelli, M. H.; Benítez, G.; Rubert, A. A.; Salvarezza, R. C. The Chemistry of the Sulfur-Gold Interface: In Search of a Unified Model. *Acc. Chem. Res.* **2012**, *45* (8), 1183–1192.

## Recommended by ACS

### Triple Amplification Ratiometric Electrochemical Aptasensor for CA125 Based on H-Gr/SH-β-CD@PdPtNFs

Guojuan Zhang, Yujing Guo, *et al.*

DECEMBER 28, 2022

ANALYTICAL CHEMISTRY

READ 

### l-Phenylalanine-Imprinted Electrochemical Sensor Based on WS<sub>2</sub> Nanoflowers on N,B-Doped Graphene and Its Application to Milk Samples

Melike Yıldırım, Mehmet Lütfi Yola, *et al.*

OCTOBER 04, 2022

INDUSTRIAL & ENGINEERING CHEMISTRY RESEARCH

READ 

### Simultaneous Determination of Ascorbic Acid, Dopamine, Uric Acid, and Acetaminophen on N, P-Doped Hollow Mesoporous Carbon Nanospheres

Mallappa Mahanthappa, Sakkarapalayam Murugesan Senthil Kumar, *et al.*

DECEMBER 08, 2022

ACS APPLIED NANO MATERIALS

READ 

### Robust Electrochemical Sensors for Detection of Isoprenaline Using Hexagonal Co<sub>3</sub>O<sub>4</sub> Nanoplates Embedded in Few-Layer Ti<sub>3</sub>C<sub>2</sub>T<sub>x</sub> Nanosheets

Jai Kumar, Selcan Karakuş, *et al.*

AUGUST 15, 2022

ACS APPLIED NANO MATERIALS

READ 

Get More Suggestions >